Thermochromic Crystals of the CT Complex between *N*-Salicylidene-2-aminopyridine and 1,3,5-Trinitrobenzene

Masashi Tanaka,* Takayuki Imai,† Takehiko Goto,† Jun-ichiro Taka,†† Mitsuhiro Akamatsu,†† Setsuo Kashino,†† and Kouichi Mogi†††

Department of Natural Science Informatics, School of Informatics and Sciences, Nagoya University, Chikusa-ku, Nagoya 464-8601

†Division of Informatics for Science, Graduate School of Human Informatics, Nagoya University, Chikusa-ku, Nagoya 464-8601

††Department of Chemistry, Faculty of Science, Okayama University, Tsushima, Okayama 700-8530

†††Institute for Molecular Science, 38 Saigo-naka, Aza, Myodaiji-cho, Okazaki 444-8585

(Received May 8, 1998)

N-Salicylidene-2-aminopyridine (NSAP) and 1,3,5-trinitrobenzene (TNB) form two kind of crystalline (1/2) complexes, forms I and II. The thermochromism was observed in a charge transfer complex form I, but not in form II. The thermochromism of these crystals was studied based on the temperature dependence of the X-ray analysis and the IR and visible absorption spectra together with the theoretical analysis.

The reversible solid state photochromism of *N*-salicylideneanilines (anils) was first observed by Senier and co-workers.[1] Cohen and co-workers undertook a more systematic study of crystalline anils and confirmed that many anils are dimorphic and that two forms occasionally differ in color, yellow and orange-red.[2] They classified the crystals of these anils in two types: in the photochromic crystals (type α), the molecules are non-planar and the aniline ring lies 40 to 50° out of the plane of the salicylideneamino group and there are no close plane-to-plane contacts in the crystal; in the thermochromic crystals (type β), the molecules are planar and packed with a plane-to-plane spacing of about 3.4 Å while displaced relative to one another along the long molecular axis. Further, in order to interpret the phenomena of photochromism and thermochromism, they proposed an intramolecular proton transfer mechanism from the enol form (OH form) to the *cis*-keto form (NH form), as is shown in Scheme 1.

Hadjoudis, Moustakali-Mavridis, and co-workers extended the structural studies in the series of heterocyclic anils like *N*-salicylidene-2-aminopyridines (NSAP).[3,4] They interpreted the thermochromic phenomenon of the crystals of NSAP derivatives as due to a shift in the tautomeric equilibrium between the enol form and the *cis*-keto form, as is shown in Scheme 2, and determined the energy difference between the colored and non-colored forms of crystalline 5-bromosalicylidene-2-aminopyridine to be 9.08 kJ mol^{-1} from the temperature dependence of the optical density of the maximum peak of the thermochromic band near 300 nm.

Bullock and co-woerkers determined the crystal structure of the Schiff base of dinitrato[*N*,*N*′-propane-1,3-diylbis(salicylideneimine)]calcium(II). The Schiff base is present in a hitherto unreported charge-separated form of salicylideneimine group with the ligand bridging two Ca ions through negatively charged O atoms. They found that the previously unconsidered, charge-separated tautomer of salicylideneimine group predominates in the complexes.[5] Kamwaya and Khoo studied the molecular adduct of dimethyltin dichloride with a salicylideneaniline derivative, 2-(*p*-methoxyphenyl iminomethyl)phenol, by X-ray analysis. They reported the unusual occurrence of the planar zwitterion of salicylidene-

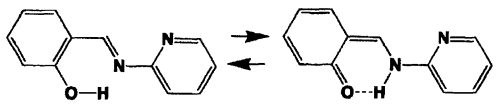

Scheme 2.

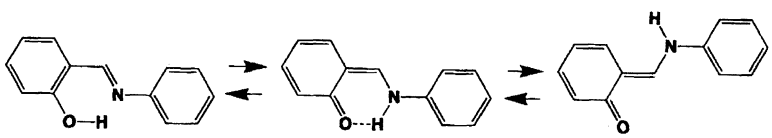

Scheme 1.

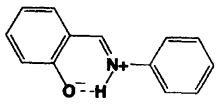

Scheme 3.

anilines as a neutral ligand, as is shown in Scheme 3.[6] Such a zwitterion was previously suggested to exist as an intermediate in the photochromic process by the optical study.[7,8]

Inabe and co-workers prepared many compounds of the *N*-salicylideneaniline family and studied the structural and optical properties in the crystalline state.[9] They found that the intramolecular hydrogen-bonded structure in *N*-(2-hydroxy-1-naphthylmethylene)aniline type compounds is an average of O–H···N and O···H–N and the potential of the proton in the hydrogen bond becomes close to a symmetrical double-well with a small energy barrier.[10] Further, they suggested that a hydrogen-bonded system with a charge-transfer (CT) interaction in accompanied by a configurational charge of the π-electron structure and the potential energy surface of the proton is modified by the intermolecular CT interaction.[11]

In our preceding papers, we showed the thermochromism in a few organic solid phases. The irreversible thermochromism of the crystals of 2,3-bis(phenylthio)-1,4-naphthoquinone changes the violet form to the red form.[12] On the other hand, the color of the crystal of 2,3-(*p*-chlorophenylthio)-1,4-naphthoquinone changes from red to dark red by heating.[13] The yellow and green forms of picrate salts with 2-iodoaniline show the thermochromism and change to the red crystal upon heating.[14] Further, the crystals of picrate with 1-bromo-2-naphthylamine showed a complicated solid phase transition.[15] We are interested in the mechanism of the phase transition of such organic molecular aggregates, because many organic compounds with the properties of the phase transition have possible applications to molecular devices or indicators.

In the present paper, we report the reversible thermochromism and the crystal structures of the complex of NSAP with 1,3,5-trinitrobenzene (TNB), and discuss the mechanism of the thermochromism by the measurement of the variable temperature visible absorption spectra together with some theoretical analysis. The crystal structure of NSAP[4] was also refined based on new diffraction data.

Experimental

Synthesis. NSAP was prepared by a well-known method.[16] The crystals of the complex of NSAP with TNB were obtained as yellowish orange prisms (form I) and orange plates (form II) from the chloroform solution. The color of the form I changes from yellowish orange to pale green by cooling, but the form II does not show any thermochromism.

Measurements. The visible absorption spectra of the single crystals of the NSAP/TNB complex were taken using an absorption microphotometer made in our laboratory. The cooling plate of LINKAM was used on measuring the temperature dependence of the absorption spectra.

X-Ray Structure Analysis. The reflection data of forms I and II of NSAP/TNB complex and NSAP at room temperatures were measured on a Rigaku AFC-5R four circle diffractometer. Low-temperature diffraction experiments on form I were carried out using a Huber off-center four-circle diffractometer. The temperatures were regulated within ±0.3 K using a closed-cycle He refrigerator (Cryogenics, HC-2) equipped with a temperature controller (Cino, KP1000). The cell constants were determined over the temperature range of 296 to 60 K. The reflection data were collected at 80 K. The crystal data and experimental details are listed in Table 1.

The structures were solved by a direct method MITHRIL[17] and refined by a full-matrix least-squares method. The quantity minimized was $\Sigma w(|F_o| - |F_c|)^2$, where $w = 1/\sigma^2(F_o)$. A difference Fourier map for the 80 K data of form I showed a peak near N8 at the stage of $R = 0.10$. The peak was higher than that observed usually for H atoms; the distance from N8 to the peak was 1.24 Å. The structure was refined by assuming a disorder in NSAP moiety, in such a way as the moiety had a pseudo two-fold axis through a center of the N7–C13 bond and perpendicular to the mean plane of the moiety. The occupancy factor of disordered O8* atom was estimated to be 0.15 from difference Fourier maps, the value of displacement parameter and the *R* value. All non-H atoms except O8* was refined anisotropically, and O8* and H atoms isotropically. Difference Fourier maps after the refinements still showed residual electron density near N7. The occupancy factor of H atom attached to N7 was further adjusted. The residual electron density near N7 became zero, when the occupancy factor of the H atom was 0.30. A difference Fourier map for the 296 K data of form I also showed a peak near N8 similar to that found for the 80 K data. The structure was refined by the same manner as adopted for the 80 K data. The occupancy factor of disordered O8* atom was estimated to be 0.15. The residual electron density near N7 became zero, when the occupancy factor of the H atom attached to N7 was 0.35.

The NSAP moiety in form II was disordered around the center of symmetry. Non-H atoms were refined anisotropically. The H atoms were found from a difference Fourier map. The positional parameters of the H atoms were fixed, and the values of the displacement parameters adopted were the same as the equivalent isotropic displacement parameters of the atoms to which they were attached. The crystal structure of NSAP was refined by using a larger number of reflections than reported previously.[4] In the present refinements, the H atoms were refined isotropically, in addition to the anisotropic refinement of the non-H atoms. A difference Fourier map was calculated after the refinements by excluding the H atom of the hydroxy group. The map showed an electron distribution elongated toward the N atom. However, the disordering of the H atom was not taken into account in the refinements, because the residual electron density near the N atom was as small as 0.2 e Å^{-3}.

Atomic scattering factors were taken from International Tables for X-Ray Crystallography.[18] Computations were carried out by using TEXSAN[19] at the X-Ray Laboratory of Okayama University. The final atomic parameters are given in Table 2.[20]

Theoretical Analysis. All ab initio molecular orbital calculations were performed with the GAUSSIAN 94 program.[21] The numerical calculations were carried out on IBM RS/6000 590 and SP2 parallel computers and NEC SX-3 supercomputer at the Institute for Molecular Science (IMS) computer center. The geometries of these two isomers were fully optimized at the RHF/3-21G* level and one point calculations were performed with the second order-Møller–Plesset (MP2) with 3-21G* basis on the optimized geometry.

Table 1. Crystal Data and Experimental Details

	NSAP/TNB $C_{12}H_{10}N_2O \cdot 2C_6H_3N_3O_6$ F.W.=624.44			NSAP $C_{12}H_{10}N_2O$ M_r=198.22
	Form I	Form I	Form II	
Temperature/K	296	80	296	296
Color	Yellow-orange	Pale green	Orange	Orange
Crystal shape	Prism	Prism	Plate	Plate
Crystal system	Triclinic	Triclinic	Monoclinic	Orthorhombic
Space group	$P\bar{1}$	$P\bar{1}$	$P2_1/c$	$Pbca$
a/Å	11.288(2)	11.087(4)	6.893(5)	14.810(4)
b/Å	14.735(3)	14.595(3)	7.498(2)	21.838(8)
c/Å	8.111(4)	8.003(4)	26.30(1)	6.318(2)
α/°	90.17(3)	90.04(3)		
β/°	93.05(3)	91.86(3)	91.1(1)	
γ/°	95.51(2)	95.33(2)		
V/Å^3	1341.0(7)	1288.6(8)	1359(2)	2043(1)
Z	2	2	2	8
D_x/Mg m^{-3}	1.546	1.609	1.526	1.288
F(000)	640	640	640	832
Radiation	Mo $K\alpha$	Mo $K\alpha$	Mo $K\alpha$	Mo $K\alpha$
λ/Å	0.71073	0.71073	0.71073	0.71073
μ/mm^{-1}	0.121	0.126	0.119	0.079
Crystal size/mm	0.58 × 0.28 × 0.28	0.58 × 0.28 × 0.28	0.45 × 0.44 × 0.15	0.54 × 0.38 × 0.14
Cell dimensions				
2θ range/°	21—22	21—23	16—22	20—22
No. of refs.	25	25	22	25
Scan mode	2θ–ω	2θ–ω	2θ–ω	2θ–ω
Scan speed ω/° min^{-1}	6	4	4	6
Scan width $\Delta\omega$/°	1.68+0.38tan θ	1.68+0.38tan θ	0.73+0.30tan θ	1.57+0.30tan θ
$2\theta_{max}$/°	52	55	52	52
hkl_{min}—hkl_{max}	0—13, −17—17, −9—9	−14—14, −18—18, 0—10	0—8, 0—9, −32—32	0—18, −1—26, 0—7
Standard refs.	3 (every 97 refs.)	3 (every 97 refs.)	3 (every 97 refs.)	3 (every 97 refs.)
Intensity variation	0.996—1.003	0.989—1.030	0.994—1.005	0.995—1.001
Measured refs.	5002	5976	2920	2098
Independent refs.	4725	5649	2704	2036
Observed refs.	3154	4471	1514	1162
	($I > 2.0\sigma(I)$)	($I > 2.0\sigma(I)$)	($I > 2.0\sigma(I)$)	($I > 1.0\sigma(I)$)
R_{int}	0.018	0.072	0.010	0.018
Extinction coef.	6.94×10^{-7}	—	5.51×10^{-7}	8.02×10^{-7}
Parameters refined	476	478	209	177
R	0.044	0.053	0.062	0.081
R_w	0.032	0.054	0.061	0.066
S	1.55	1.37	1.79	1.18
Least squares weight	$1/\sigma(F_o)^2$	$1/\sigma(F_o)^2$	$1/\sigma(F_o)^2$	$1/\sigma(F_o)^2$
$(\Delta/\sigma)_{max}$	0.037	0.089	0.029	0.003
$(\Delta\rho)_{max}$, $(\Delta\rho)_{min}$/eÅ^{-3}	0.21, −0.15	0.33, −0.42	0.39, −0.26	0.22, −0.26

Results and Discussion

Crystal and Molecular Structures. (a) Form I. The temperature dependence of cell constants is shown in Fig. 1. The cell constants monotonically decrease upon cooling from 296 to 80 K and increase upon heating from 60 to 296 K. The cell constants at 296 K before and after cooling are in agreement within the experimental errors. The temperature dependence shows that the crystal structures at 296 and 80 K are isostructural.

The ORTEP drawing[22] is shown in Fig. 2, along with the numbering of atoms. The numbering scheme for NSAP molecule refers to the major one with the occupancy factor of 0.85. The asymmetric unit consists of one NSAP molecule and two TNB molecules. The bond lengths and angles are listed in Table 3. The N–O lengths in the nitro groups are underestimated at 296 K because of large thermal vibration of the O atoms. Although the NSAP molecule is disordered, the bond lengths observed reflect structural features characteristic of N-salicylideneaniline derivatives.[10] The C8–O8 and C13–N7 lengths at 298 and 80 K are comparable with those found in *N*-tetrachlorosalicylideneaniline, showing a contribution of the keto form to the structure.[9] A bond-length alternation expected for a quinonoid structure was observed in the

Table 2. Positional Parameters and Equivalent Displacement Parameters (U_{eq}) for Non-H atoms

Atom	x	y	z	U_{eq}/Å
(1) Form I, 296 K				
O1	0.4213(2)	0.1850(1)	−0.0467(3)	0.103(1)
O2	0.2532(2)	0.1361(1)	−0.1651(3)	0.100(1)
O3	−0.0183(2)	0.3579(1)	−0.3410(2)	0.082(1)
O4	−0.0097(2)	0.4841(1)	−0.2060(3)	0.095(1)
O5	0.3338(2)	0.5745(1)	0.1578(3)	0.090(1)
O6	0.4760(2)	0.4878(1)	0.1818(2)	0.072(1)
O1b	−0.0835(2)	0.0049(1)	0.6408(2)	0.079(1)
O2b	0.0005(2)	0.1414(1)	0.6198(3)	0.089(1)
O3b	−0.2088(2)	0.3700(1)	0.3456(3)	0.105(1)
O4b	−0.3694(2)	0.3319(1)	0.2006(3)	0.100(1)
O5b	−0.5371(2)	0.0183(1)	0.1868(3)	0.120(1)
O6b	−0.4728(2)	−0.0747(1)	0.3640(2)	0.073(1)
O8	0.2627(3)	0.1597(2)	0.3314(4)	0.073(1)
O8*	−0.074(1)	0.340(1)	0.053(2)	0.085(4)
N1	0.3214(2)	0.1954(1)	−0.0997(3)	0.068(1)
N2	0.0286(2)	0.4124(2)	−0.2399(3)	0.060(1)
N3	0.3782(2)	0.5050(1)	0.1286(3)	0.056(1)
N1b	−0.0813(2)	0.0829(2)	0.5916(3)	0.061(1)
N2b	−0.2883(2)	0.3143(2)	0.2936(3)	0.070(1)
N3b	−0.4666(2)	−0.0021(2)	0.2929(3)	0.066(1)
N7	0.0614(2)	0.2075(1)	0.1942(2)	0.054(1)
N8	−0.0912(2)	0.2594(1)	0.0161(3)	0.062(1)
C1	0.2799(2)	0.2870(2)	−0.0861(3)	0.047(1)
C2	0.1747(2)	0.3046(2)	−0.1684(3)	0.048(1)
C3	0.1396(2)	0.3905(2)	−0.1507(3)	0.046(1)
C4	0.2032(2)	0.4576(2)	−0.0546(3)	0.047(1)
C5	0.3072(2)	0.4355(2)	0.0229(3)	0.043(1)
C6	0.3488(2)	0.3514(2)	0.0095(3)	0.047(1)
C1b	−0.1851(2)	0.1076(2)	0.4885(3)	0.046(1)
C2b	−0.1877(2)	0.1973(2)	0.4439(3)	0.049(1)
C3b	−0.2830(2)	0.2187(2)	0.3447(3)	0.048(1)
C4b	−0.3736(2)	0.1542(2)	0.2904(3)	0.054(1)
C5b	−0.3669(2)	0.0665(2)	0.3431(3)	0.047(1)
C6b	−0.2740(2)	0.0405(2)	0.4418(3)	0.049(1)
C7	0.1968(2)	0.3086(2)	0.3582(3)	0.047(1)
C8	0.2779(2)	0.2448(2)	0.3880(3)	0.051(1)
C9	0.3824(3)	0.2700(2)	0.4813(4)	0.063(1)
C10	0.4067(3)	0.3571(2)	0.5436(3)	0.065(3)
C11	0.3261(3)	0.4204(2)	0.5156(3)	0.061(1)
C12	0.2225(3)	0.3963(2)	0.4237(3)	0.054(1)
C13	0.0891(2)	0.2872(2)	0.2565(3)	0.047(1)
C14	−0.0445(2)	0.1892(2)	0.0904(3)	0.049(1)
C15	−0.0937(2)	0.1001(2)	0.0709(3)	0.056(1)
C16	−0.1976(3)	0.0827(2)	−0.0242(3)	0.065(1)
C17	−0.2490(3)	0.1538(2)	−0.0993(3)	0.063(1)
C18	−0.1928(3)	0.2400(2)	−0.0784(3)	0.065(3)
(2) Form I, 80 K				
O1	0.4322(2)	0.1830(1)	−0.0551(2)	0.025(1)
O2	0.2582(2)	0.1312(1)	−0.1683(2)	0.024(1)
O3	−0.0172(2)	0.3569(1)	−0.3447(2)	0.0201(9)
O4	−0.0122(2)	0.4839(1)	−0.2030(2)	0.026(1)
O5	0.3329(2)	0.5739(1)	0.1650(2)	0.0232(9)
O6	0.4804(1)	0.4862(1)	0.1829(2)	0.0184(9)
O1b	−0.0827(2)	0.0012(1)	0.6425(2)	0.0201(9)
O2b	0.0043(2)	0.1401(1)	0.6202(2)	0.024(1)
O3b	−0.2035(2)	0.3724(1)	0.3403(2)	0.028(1)
O4b	−0.3636(2)	0.3335(1)	0.1851(2)	0.025(1)
O5b	−0.5387(2)	0.0175(1)	0.1809(3)	0.035(1)
O6b	−0.4766(2)	−0.0757(1)	0.3687(2)	0.0185(9)
O8	0.2689(3)	0.1593(1)	0.3260(3)	0.017(1)
O8*	−0.074(1)	0.345(1)	0.047(2)	0.033(4)
N1	0.3283(2)	0.1925(1)	−0.1056(3)	0.017(1)
N2	0.0284(2)	0.4117(1)	−0.2399(3)	0.016(1)
N3	0.3798(2)	0.5037(1)	0.1315(2)	0.014(1)
N1b	−0.0791(2)	0.0808(1)	0.5920(2)	0.016(1)
N2b	−0.2828(2)	0.3157(1)	0.2844(3)	0.018(1)
N3b	−0.4683(2)	−0.0030(1)	0.2919(3)	0.018(1)
N7	0.0646(2)	0.2074(1)	0.1909(3)	0.016(1)
N8	−0.0885(2)	0.2616(1)	0.0102(3)	0.018(1)
C1	0.2855(2)	0.2848(2)	−0.0889(3)	0.013(1)
C2	0.1780(2)	0.3022(2)	−0.1713(3)	0.013(1)
C3	0.1412(2)	0.3890(2)	−0.1510(3)	0.013(1)
C4	0.2035(2)	0.4571(2)	−0.0541(3)	0.013(1)
C5	0.3103(2)	0.4346(2)	0.0242(3)	0.012(1)
C6	0.3545(2)	0.3495(2)	0.0074(3)	0.013(1)
C1b	−0.1828(2)	0.1064(2)	0.4870(3)	0.013(1)
C2b	−0.1838(2)	0.1975(2)	0.4409(3)	0.013(1)
C3b	−0.2800(2)	0.2190(2)	0.3377(3)	0.013(1)
C4b	−0.3716(2)	0.1547(2)	0.2830(3)	0.014(1)
C5b	−0.3666(2)	0.0660(2)	0.3389(3)	0.013(1)
C6b	−0.2732(2)	0.0385(2)	0.4416(3)	0.013(1)
C7	0.1986(2)	0.3100(2)	0.3579(3)	0.012(1)
C8	0.2837(2)	0.2452(2)	0.3859(3)	0.013(1)
C9	0.3893(2)	0.2707(2)	0.4792(4)	0.016(1)
C10	0.4129(2)	0.3583(2)	0.5434(3)	0.016(3)
C11	0.3295(2)	0.4233(2)	0.5169(3)	0.015(1)
C12	0.2237(2)	0.3988(2)	0.4252(3)	0.014(1)
C13	0.0905(2)	0.2881(2)	0.2553(3)	0.012(1)
C14	−0.0413(2)	0.1898(2)	0.0867(3)	0.013(1)
C15	−0.0914(2)	0.0993(2)	0.0675(3)	0.014(1)
C16	−0.1966(2)	0.0810(2)	−0.0280(3)	0.016(1)
C17	−0.2482(2)	0.1546(2)	−0.1064(3)	0.016(1)
C18	−0.1905(2)	0.2418(2)	−0.0859(3)	0.018(3)
(3) Form II				
O1	0.4711(5)	0.1147(6)	0.2450(1)	0.147(3)
O2	0.6556(5)	0.2255(5)	0.3029(1)	0.137(3)
O3	0.4723(5)	0.1978(5)	0.4777(1)	0.132(3)
O4	0.1976(6)	0.0879(6)	0.4964(1)	0.160(4)
O5	−0.2322(5)	−0.1326(5)	0.3636(2)	0.141(3)
O6	−0.1303(5)	−0.1435(5)	0.2862(2)	0.451(3)
O8	−0.1942(7)	0.4057(7)	0.4171(2)	0.095(4)
N1	0.5107(6)	0.1519(5)	0.2887(2)	0.099(3)
N2	0.3216(6)	0.1295(5)	0.4667(1)	0.101(3)
N3	−0.1120(6)	−0.1056(5)	0.3314(2)	0.113(4)
C1	0.3710(5)	0.1015(5)	0.3278(1)	0.073(3)
C2	0.4136(5)	0.1373(5)	0.3777(2)	0.075(3)
C3	0.2760(6)	0.0905(5)	0.4125(1)	0.077(3)
C4	0.0990(5)	0.0127(5)	0.3990(1)	0.080(3)
C5	0.0687(5)	−0.0202(5)	0.3481(2)	0.079(3)
C6	0.2013(6)	0.0235(5)	0.3120(1)	0.082(3)
C7	0.1143(5)	0.5288(5)	0.4383(1)	0.076(3)
C8	−0.0211(5)	0.4733(5)	0.4039(1)	0.068(3)
C9	0.0194(6)	0.4763(5)	0.3544(2)	0.090(3)
C10	0.1937(7)	0.5352(5)	0.3366(1)	0.087(3)
C11	0.3375(5)	0.5896(5)	0.3710(2)	0.087(3)
C12	0.2965(6)	0.5870(5)	0.4216(1)	0.081(3)
C13	0.0802(4)	0.5285(4)	0.4913(1)	0.067(3)

Table 2. (Continued)

Atom	x	y	z	U_{eq}/Å	Atom	x	y	z	U_{eq}/Å
					C5	0.2234(3)	0.1100(3)	1.0656(8)	0.085(4)
(4) NSAP					C6	0.2053(3)	0.0659(2)	0.9195(8)	0.081(4)
O1	0.1327(2)	0.0346(1)	0.6045(5)	0.087(3)	C7	0.0494(2)	0.1508(2)	0.5570(6)	0.056(3)
N1	0.0292(2)	0.1117(1)	0.4142(5)	0.061(3)	C8	−0.0286(2)	0.1272(2)	0.2455(6)	0.058(3)
N2	−0.0581(2)	0.1848(1)	0.2271(5)	0.072(3)	C9	−0.0524(3)	0.0811(2)	0.1058(7)	0.072(3)
C1	0.1488(2)	0.0791(2)	0.7493(7)	0.063(3)	C10	−0.1074(3)	0.0948(2)	−0.0596(8)	0.081(4)
C2	0.1098(2)	0.1368(2)	0.7287(6)	0.056(3)	C11	−0.1388(3)	0.1529(2)	−0.0840(8)	0.082(4)
C3	0.1301(3)	0.1805(2)	0.8828(7)	0.071(3)	C12	−0.1125(3)	0.1961(2)	0.0604(8)	0.081(4)
C4	0.1869(3)	0.1682(2)	1.0476(7)	0.081(4)					

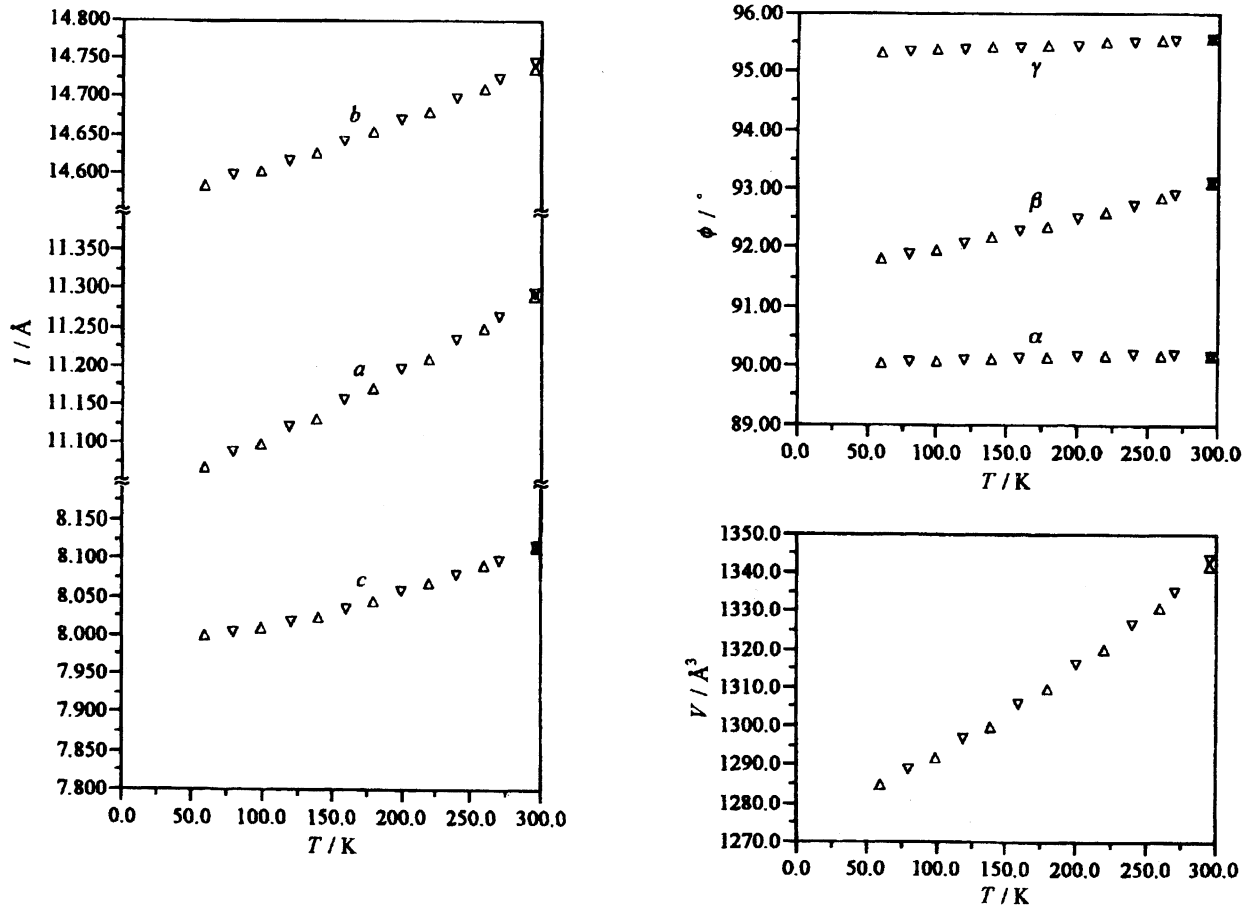

Fig. 1. The temperature dependence of the cell constants (*a*, *b*, *c*, and *V*) of form I. The values obtained on cooling are shown by triangles with the bottom up, and those on heating by triangles with the bottom down.

benzene ring at 80 K. The short O8*–C8* distances at both temperatures suggest that the NSAP molecule with a low occupancy factor takes a keto form. No significant differences were observed for the bond angles and molecular conformations between two temperatures. The NSAP molecule is distorted from a planar structure: The torsion angles C7–C13–N7–C14, N7–C13–C7–C8, and C13–N7–C14–C15 are −178.3(2), 2.5(4), and −158.2(2)° at 296 K; −178.2(2), 3.0(4), and −157.4(2)° at 80 K. The temperature has also no influence on the O8···N7 distance in the hydrogen-bonded chelate ring: 2.629(3) Å at 296 K and 2.632(3) Å at 80 K. The distance is longer than those found in the CT complexes of anil derivatives.[11]

The difference Fourier maps at 296 and 80 K are shown in Fig. 3; which they were calculated by eliminating the H atoms attached to O8 and N7 from the refined structure. At both temperatures the sub peak appears near N7. This peak did not disappear when an H atom was attached to N7 with the occupancy factor of 0.15. This value corresponds to the occupancy factor of the H atom of disordered C13* which occupies the same position as N7. The residual electron density of the sub peak became zero when the occupancy factor of the H atom was increased to 0.30 at 80 K and 0.35 at 296 K. The results indicate a contribution of the keto form to the major molecule of NSAP in accordance with the indication from the C–O bond length. Quantitative discussion on the contribution of the keto form is limited by the precision of the diffraction data. The distances between

Table 3. Bond Lengths (l) and Angles (φ) of Form I

	296 K	80 K		296 K	80 K
	l/Å	l/Å		l/Å	l/Å
O1–N1	1.209(3)	1.229(3)	C1–C2	1.378(3)	1.387(3)
O2–N1	1.210(3)	1.225(3)	C1–C6	1.377(3)	1.377(3)
O3–N2	1.210(2)	1.222(3)	C2–C3	1.372(3)	1.378(3)
O4–N2	1.215(2)	1.224(3)	C3–C4	1.379(3)	1.379(3)
O5–N3	1.210(2)	1.225(3)	C4–C5	1.369(3)	1.388(3)
O6–N3	1.214(2)	1.226(2)	C5–C6	1.373(3)	1.386(3)
O1b–N1b	1.216(2)	1.229(2)	C1b–C2b	1.374(3)	1.381(3)
O2b–N1b	1.212(2)	1.221(2)	C1b–C6b	1.377(3)	1.382(3)
O3b–N2b	1.214(3)	1.224(3)	C2b–C3b	1.370(3)	1.387(3)
O4b–N2b	1.203(3)	1.224(3)	C3b–C4b	1.380(3)	1.378(3)
O5b–N3b	1.199(3)	1.220(3)	C4b–C5b	1.369(3)	1.376(3)
O6b–N3b	1.214(2)	1.225(3)	C5b–C6b	1.370(3)	1.389(3)
O8–C8	1.327(3)	1.335(3)	C7–C8	1.387(3)	1.410(3)
O8*–N8	1.23(1)	1.24(1)	C7–C12	1.394(3)	1.403(3)
N1–C1	1.476(3)	1.476(3)	C7–C13	1.441(3)	1.442(3)
N2–C3	1.477(3)	1.483(3)	C8–C9	1.387(3)	1.389(3)
N3–C5	1.480(3)	1.469(3)	C9–C10	1.374(4)	1.376(3)
N1b–C1b	1.478(3)	1.478(3)	C10–C11	1.376(4)	1.397(3)
N2b–C3b	1.476(3)	1.478(3)	C11–C12	1.370(3)	1.381(3)
N3b–C5b	1.478(3)	1.479(3)	C14–C15	1.381(3)	1.392(3)
N7–C13	1.281(3)	1.289(3)	C15–C16	1.372(3)	1.379(3)
N7–C14	1.429(3)	1.421(3)	C16–C17	1.375(4)	1.402(3)
N8–C14	1.335(3)	1.352(3)	C17–C18	1.369(3)	1.378(3)
N8–C18	1.351(3)	1.355(3)			
	φ/°	φ/°		φ/°	φ/°
O1–N1–O2	124.5(2)	124.7(2)	C4–C5–C6	123.4(2)	123.2(2)
O1–N1–C1	118.1(2)	117.2(2)	C1–C6–C5	117.0(2)	116.9(2)
O2–N1–C1	117.4(2)	118.0(2)	N1b–C1b–C2b	117.9(2)	117.6(2)
O3–N2–O4	124.5(2)	124.8(2)	N1b–C1b–C6b	119.0(2)	118.6(2)
O3–N2–C3	118.0(2)	117.7(2)	C2b–C1b–C6b	123.1(2)	123.8(2)
O4–N2–C3	117.5(2)	117.5(2)	C1b–C2b–C3b	117.1(2)	116.4(2)
O5–N3–O6	124.6(2)	124.6(2)	N2b–C3b–C2b	118.5(2)	117.8(2)
O5–N3–C5	117.6(2)	118.0(2)	N2b–C3b–C4b	118.9(2)	119.1(2)
O6–N3–C5	117.7(2)	117.4(2)	C2b–C3b–C4b	122.5(2)	123.2(2)
O1b–N1b–O2b	124.7(2)	125.0(2)	C3b–C4b–C5b	117.3(2)	117.0(2)
O1b–N1b–C1b	117.5(2)	117.4(2)	N3b–C5b–C4b	117.8(2)	118.1(2)
O2b–N1b–C1b	117.8(2)	117.6(2)	N3b–C5b–C6b	119.1(2)	118.3(2)
O3b–N2b–O4b	124.1(2)	124.3(2)	C4b–C5b–C6b	123.1(2)	123.5(2)
O3b–N2b–C3b	117.7(2)	118.0(2)	C1b–C6b–C5b	116.8(2)	116.0(2)
O4b–N2b–C3b	118.2(2)	117.6(2)	C8–C7–C12	119.0(2)	118.7(2)
O5b–N3b–O6b	124.5(2)	124.8(2)	C8–C7–C13	121.5(2)	121.3(2)
O5b–N3b–C5b	117.7(2)	117.4(2)	C12–C7–C13	119.5(2)	119.9(2)
O6b–N3b–C5b	117.8(2)	117.7(2)	O8–C8–C7	124.0(2)	123.4(2)
C13–N7–C14	120.2(2)	119.6(2)	O8–C8–C9	116.8(3)	117.4(2)
O8*–N8–C14	128.1(6)	128.9(6)	C7–C8–C9	119.2(2)	119.3(2)
O8*–N8–C18	112.1(6)	111.4(6)	C8–C9–C10	121.0(3)	121.3(2)
C14–N8–C18	116.8(2)	116.6(2)	C9–C10–C11	120.1(3)	120.2(2)
N1–C1–C2	119.1(2)	118.4(2)	C10–C11–C12	119.5(3)	119.3(2)
N1–C1–C6	118.0(2)	118.3(2)	C7–C12–C11	121.3(3)	121.3(2)
C2–C1–C6	122.8(2)	123.3(2)	N7–C13–C7	121.8(2)	121.7(2)
C1–C2–C3	116.9(2)	116.3(2)	N7–C14–C8	118.3(2)	118.7(2)
N2–C3–C2	118.4(2)	118.4(2)	N7–C14–C15	118.6(2)	118.4(2)
N3–C3–C4	118.3(2)	117.5(2)	N8–C14–C15	123.0(2)	123.0(2)
C2–C3–C4	123.2(2)	124.1(2)	C14–C15–C16	118.8(3)	119.3(2)
C3–C4–C5	116.7(2)	116.2(2)	C15–C16–C17	119.3(3)	118.6(2)
N3–C5–C4	118.7(2)	118.8(2)	C16–C17–C18	118.4(3)	118.4(2)
N3–C5–C6	117.9(2)	118.0(2)	N8–C18–C17	123.6(3)	124.0(2)

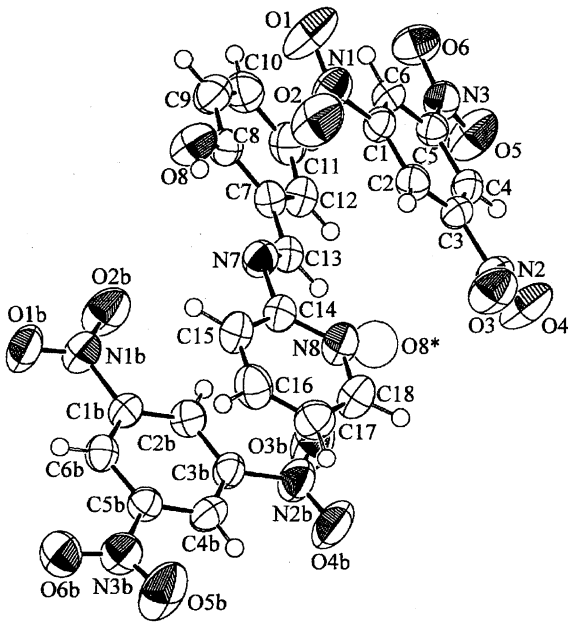

Fig. 2. The ORTEP drawing at 296 K and the numbering of atoms of form I. Disordered C8* occupies the same position as N8. The displacement ellipsoids are drawn at 50% probability level and the H atoms are drawn as spheres equivalent to $B_{iso} = 1.0$ Å^2.

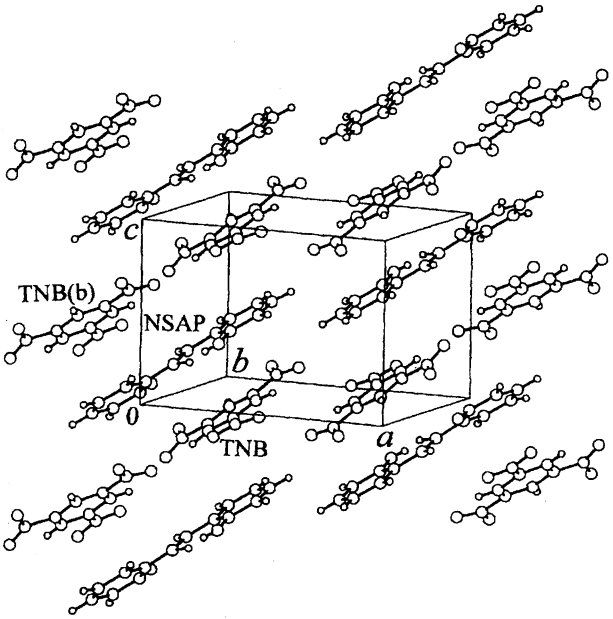

Fig. 4. A perspective view of the crystal structure of form I.

O8 and the H atom attached to it were underestimated to be 0.59(4) Å at 80 K and 0.62(3) Å at 296 K, probably because of an effect of bonding electrons, as indicated by anharmonic distribution of the electron density near O8.

A perspective view of the crystal structure is shown in Fig. 4. The structure is described based on the NSAP molecule with high occupancy factor. The donors (NSAP) and acceptors (TNB) are mixed along the stacking direction (*c* axis). The repeating unit is TNB–NSAP–TNB (b), and one NSAP is located between TNB and TNB(b) molecules. The salicylideneimine moiety of NSAP overlaps in nearly parallel with TNB, the dihedral angle between their benzene-ring planes being 3.6(3)° at 296 K and 3.8(3)° at 80 K. The pyridine ring overlaps with TNB(b), the dihedral angle between the pyridine and benzene rings being 4.3(3)° at 296 K and 4.6(3)° at 80 K. There are twelve C···C contacts between the

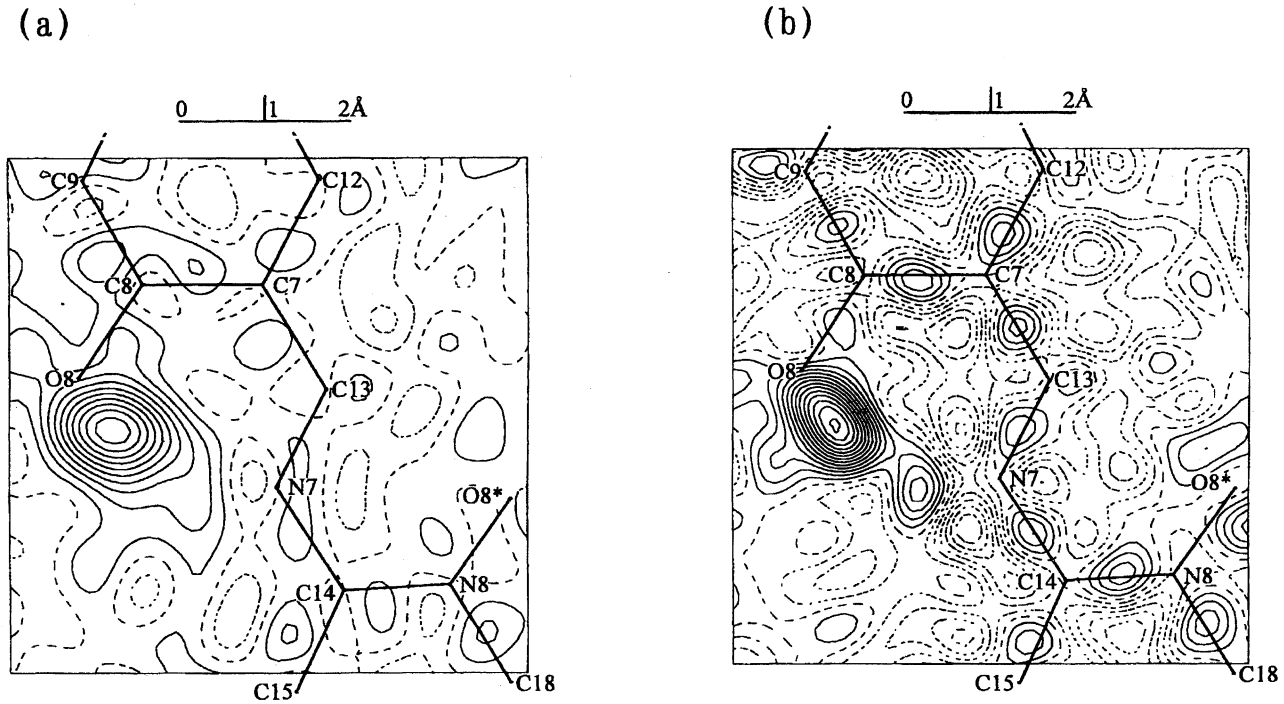

Fig. 3. The difference-Fourier maps for the section through O8, N7, and C7 at (a) 296 and (b) 80 K. Contours are drawn by solid lines (above 0.05 e Å^{-3}) and dashed lines (below −0.05 e Å^{-3}) with intervals of 0.05 e Å^{-3}.

overlapping molecules, the average distance being 3.548(4) Å at 296 K and 3.469(4) Å at 80 K. The shortest distances are 3.372(4) Å for C2b···C14 and 3.415(4) Å for C6···C7 at 296 K, which decrease to 3.296(4) and 3.365(4) Å, respectively, at 80 K. Thus, the effect of the temperatures appears in the C···C contacts.

(b) Form II. The ORTEP drawing[22] is shown in Fig. 5, along with the numbering of atoms. The molecular unit shown in Fig. 5 consists of one NSAP molecule and two TNB molecules. There is an inversion center at the center of the NSAP molecule due to the disorder of the molecule. The bond lengths and bond angles are listed in Table 4. The bond lengths in the disordered NSAP can roughly be explained as an average of the salicylideneimine and 2-aminopyridine moieties. The C8–O8 distance is slightly longer than that observed in form I. The NSAP is planar in contrast with that in form I, the tortion angle N7–C13–C7–C8 being 1.6(6)°. The O8···N7 distance, 2.567(6) Å, is shorter than that in form I, and comparable with those found in the CT complexes of anil derivatives.[11]

The crystal structure viewed along the *b* axis is shown in Fig. 6. The NSAP and TNB molecules are alternately stacked along the *b* axis. The NSAP overlaps in nearly parallel with TNB, the dihedral angle between the overlapping planes of their six-member rings being 4.7(5)°. There are nine C···C contacts between the overlapping molecules, the average distance being 3.504(5) Å. The shortest distance, 3.436(5) Å, is found for C2···C11. The average distance is shorter than that in form I at 296 K, while the shortest distance is longer.

Table 4. Bond Lengths (l) and Angles (φ) of Form II

	l/Å		l/Å
O1–N1	1.208(4)	C2–C3	1.376(5)
O2–N1	1.194(4)	C3–C4	1.392(5)
O3–N2	1.189(4)	C4–C5	1.372(5)
O4–N2	1.221(4)	C5–C6	1.371(5)
O5–N3	1.214(5)	C7–C8	1.352(5)
O6–N3	1.227(5)	C7–C12	1.408(5)
O8–C8	1.348(5)	C7–C13	1.419(5)
N1–C1	1.471(5)	C8–C9	1.338(5)
N2–C3	1.484(5)	C9–C10	1.370(5)
N3–C5	1.460(5)	C10–C11	1.389(5)
C1–C2	1.366(5)	C11–C12	1.367(5)
C1–C6	1.366(5)	C13–C13*	1.278(6)
	φ/°		φ/°
O1–N1–O2	125.0(4)	C3–C4–C5	116.1(3)
O1–N1–C1	117.8(4)	N3–C5–C4	119.0(4)
O2–N1–C1	117.2(4)	N3–C5–C6	118.2(4)
O3–N2–O4	125.4(4)	C4–C5–C6	122.8(4)
O3–N2–C3	119.1(4)	C1–C6–C5	118.0(3)
O4–N2–C3	115.5(4)	C8–C7–C12	119.7(3)
O5–N3–O6	125.4(5)	C8–C7–C13	122.1(3)
O5–N3–C5	116.9(5)	C12–C7–C13	118.2(3)
O6–N3–C5	117.7(5)	O8–C8–C7	123.2(3)
N1–C1–C2	119.3(4)	O8–C8–C9	117.3(4)
N1–C1–C6	117.8(4)	C7–C8–C9	119.4(3)
C2–C1–C6	122.9(4)	C8–C9–C10	122.5(4)
C1–C2–C3	116.7(3)	C9–C10–C11	119.5(3)
N2–C3–C2	116.9(4)	C10–C11–C12	118.1(3)
N2–C3–C4	119.7(4)	C7–C12–C11	120.7(3)
C2–C3–C4	123.4(3)	C7–C13–C13*	120.8(4)

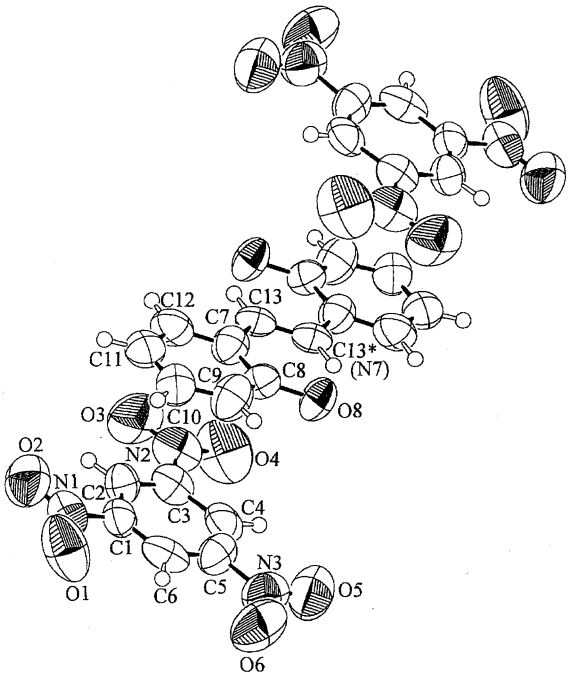

Fig. 5. The ORTEP drawing and the numbering of atoms of form II. The N7 occupies the same position as disordered C13*. The displacement ellipsoids are drawn at 50% probability level and the H atoms are drawn as spheres equivalent to $B_{iso} = 1.0$ Å^2.

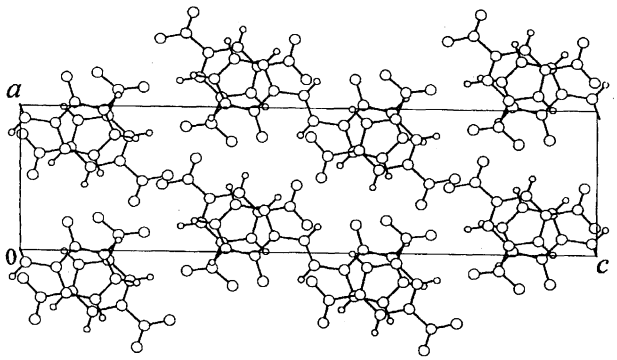

Fig. 6. The crystal structure viewed along the *b* axis of form II.

(c) Crystal Structure of NSAP. The NSAP molecule is planar, and the bond lengths in the molecule are in agreement within the experimental errors with those reported previously.[4] However, the quinonoid character appears clearly in the benzene ring in the present analysis. The phenolic C–O distance, 1.355(4) Å, is confirmed to be longer than that observed in form I and comparable with that in form II. The O···N distance, 2.575(4) Å, is comparable with that in form II.

(d) Comparison of the Structures. Crystals of form I are thermochromic, although the O···N distance in the hydrogen bonded chelate ring is significantly longer than those found in the crystals of NSAP and the CT complexes of anil

derivatives.[11] This fact shows that the thermochromism in this series of crystals is not governed only by the O···N distance. The phenolic C–O distance in form I is the shortest among those in the crystals of forms I and II, and NSAP. This contraction of the C–O bond is an indication of a large contribution of the keto form in form I. The C···C distances between the overlapping molecules in form I decrease with a decrease in temperature. This fact suggests that the interactions between the overlapping molecules in form I stabilize the keto form even at 80 K. The NSAP molecule in form II has the similar O···N distance and C–O length to those in thermochromic NSAP crystal. The difference in the thermochromic properties of these crystals cannot be explained by the difference in the molecular geometry. It is of note that the NSAP molecule in form II is disordered around an inversion center, while that in the NSAP crystal is ordered. The difference in the imino C–N distances was within 3 a.u. among the crystals of forms I and II, and NSAP.

IR-Visible Absorption and Theoretical Studies. The theoretical potential curve of the proton in NSAP is shown in Fig. 7. The enol form is more stable than the keto form. The energy difference between two forms is calculated to be 21.3 kJ mol^{-1} and the activation energy is 39:3 kJ mol^{-1}. The observed energy difference is obtained by measuring the absorption spectra of the single crystal at various temperatures and plotting log (O.D.) against $1/T$ from the absorption spectra.[3,23]

Figure 8(a) shows the spectra of the NSAP crystal at various temperatures and Fig. 8(b) depicts the variations with temperature of the optical density of the thermochromic band at 500 nm. The spectral behavior does not depend on the direction of the polarized light. The energy difference is found to be 7.5 kJ mol^{-1}. This value is comparable to the theoretical value and almost equal to the experimental value (2.17

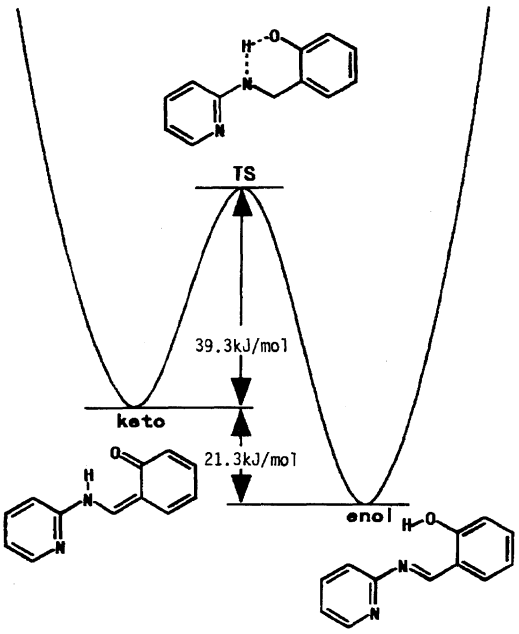

Fig. 7. The theoretical potential curve of the proton in the NSAP system.

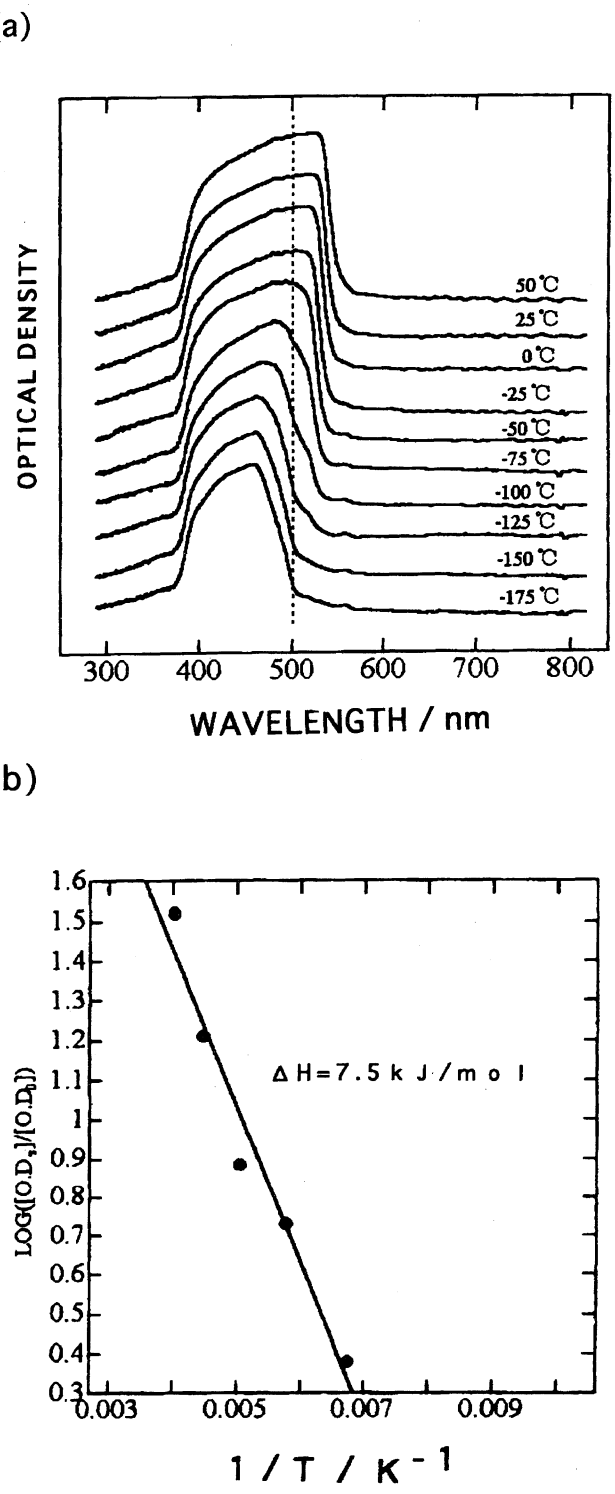

Fig. 8. (a) The absorption spectra and (b) the plot of log (O.D.) at 500 nm against $1/T$ of the thermochromic band at 500 nm of the NSAP crystal.

kcal mol^{-1} = 9.08 kJ mol^{-1}) obtained by Hadioudis and coworkers.[3] Their value was obtained by the measurement of the polycrystalline films between optical quartz plates.

The polarized absorption spectra at room temperature of the NSAP/TNB crystal (form I) are shown in Fig. 9. The spectra have two bands in the vicinity of 400 to 550 nm. The

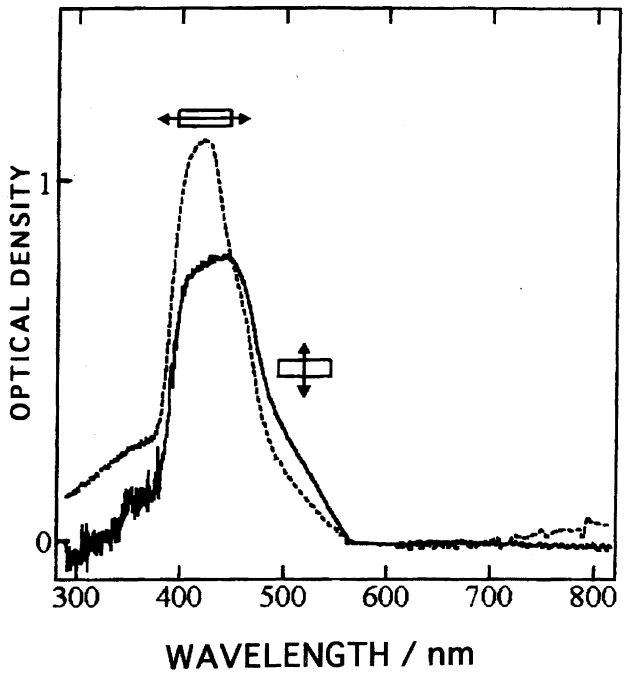

Fig. 9. The polarized absorption spectra at room temperature of the NSAP/TNB crystal (form I).

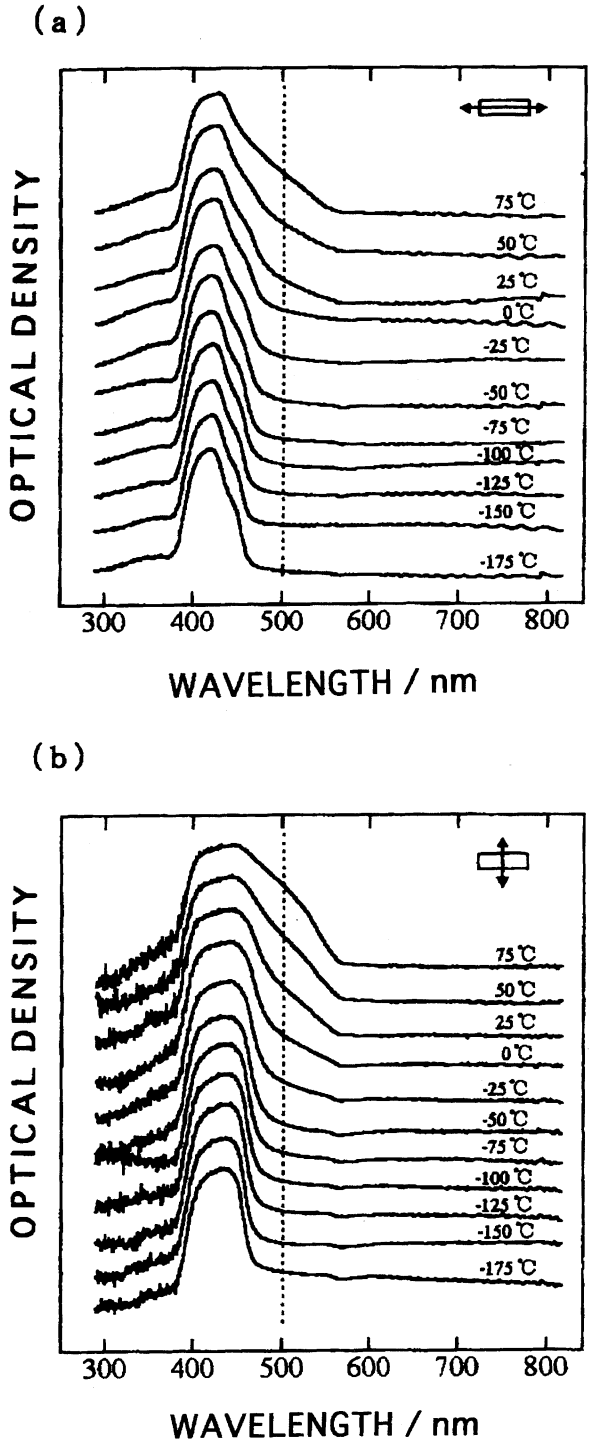

Fig. 10. The polarized absorption spectra of the NSAP/TNB crystal (form I) at various temperature for light polarized (a) parallel and (b) perpendicular to the *c* axis.

first band at 530 nm is mainly observed as the shoulder for the light polarized perpendicular to the stacking axis (*c* axis), but the second band at 430 nm is observed more intensely for the light polarized parallel to the *c* axis. That is, the first band at 530 nm can not be assigned to the CT band.

Figure 10 shows the polarized spectra of the NSAP/TNB crystal (form I) at various temperatures for the light polarized (a) parallel and (b) perpendicular to the *c* axis. The temperature dependence of the visible spectra can be mainly observed for the light polarized perpendicular to the *c* axis. This means that the origin of the thermochromism of the NSAP/TNB crystal (form I) is the same as that of the NSAP crystal. The CT band can not be observed due to the small overlap integral between the HOMO of NASP and the LUMO of TNB.[24] The plot of log (O.D.) at 500 nm against $1/T$ from the spectra for the light polarized perpendicular to the *c* axis is shown in Fig. 11. The obtained energy difference is 4.6 kJ mol^{-1}. This value is about half of the value (7.5 kJ mol^{-1}) of the NSAP crystal. This fact supports the opinion of Inabe and co-workers that the CT interaction has a great influence upon the potential curve of the proton.[9] The temperature dependencies of the IR polarized spectra are shown in Fig. 12. The intensity of the γOH band at 814 cm^{-1} increases with cooling temperature. This fact means the proton transfer in the hydrogen system occurs during the thermochromism.

Conclusion. The NSAP/TNB (form I) crystal shows the reversible thermochromism and its color changes from yellowish orange to pale green upon cooling temperature. The lattice constants decrease monotonically with cooling and the intensity variation of the thermochromic band can be interpreted by the Arrhenius relation. The intermolecular weak CT interaction modifies the potential energy curve of the proton, although the charge-transfer interaction is weak in this crystal. The component molecule (NSAP) in form I makes a great contribution of the keto form, while we can not obtain the direct proof of the proton transfer. This means that the average O–H bond length is determined by the proton population energy curve of the hydrogen-bond system and the proton transfer causes the reversible thermochromic phe-

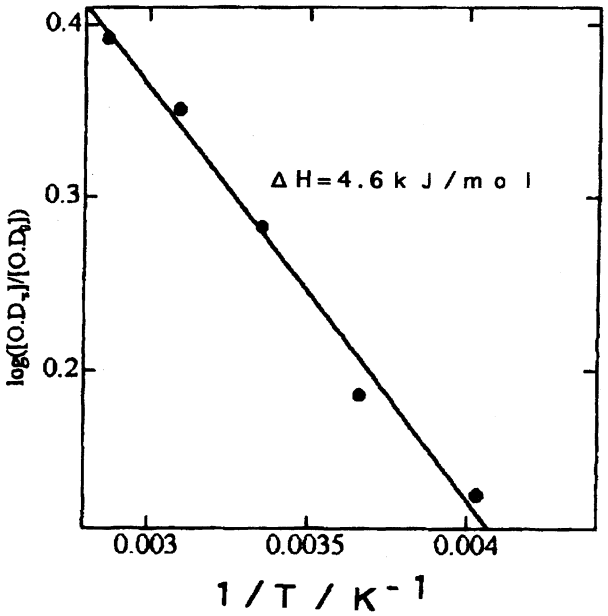

Fig. 11. The plot of log (O.D.) at 500 nm against $1/T$ of the thermochromic band of the NSAP/TNB crystal for the light polarized perpendicular to the c axis.

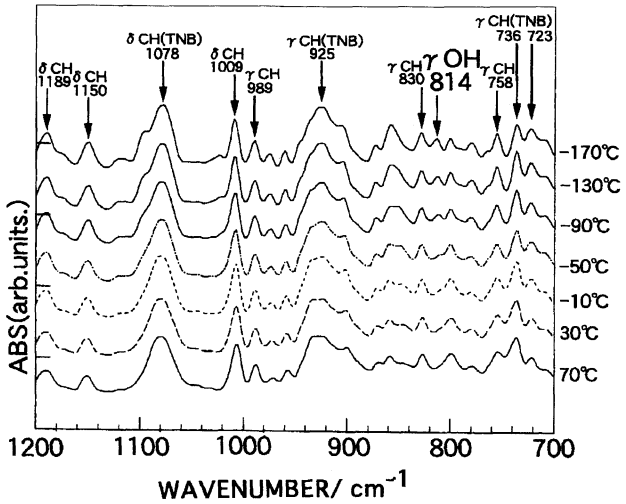

Fig. 12. The temperature dependence of the infrared spectra of the crystal (form I) of the NSAP/TNB complex.

nomenon in the solid phase under the thermal equilibrium.

References

1) A. Senier and F. G. Shepheard, *J. Chem. Soc.*, **95**, 1943 (1909); A. Senier, F. G. Shepheard, and R. Clarke, *J. Chem. Soc.*, **101**, 1952 (1912).

2) M. D. Cohen and G. M. J. Schmidt, *J. Phys. Chem.*, **66**, 2442 (1962); M. D. Cohen, G. M. J. Schmidt, and S. Flavian, *J. Chem. Soc.*, **1964**, 2041; M. D. Cohen, Y. Hirshberg, and G. M. J. Schmidt, *J. Chem. Soc.*, **1964**, 2051; J. Bregman, L. Leiserowitz, and G. M. J. Schmidt, *J. Chem. Soc.*, **1964**, 2068; M. D. Cohen and S. Flavian, *J. Chem. Soc. B*, **1967**, 334.

3) E. Hadjoudis, I. Moustakali-Mavridis, and J. Xexakis, *Isr. J. Chem.*, **18**, 202 (1979); E. Hadjoudis, M. Vitorakis, and I. Moustakali-Mavridis, *Mol. Cryst. Liq. Cryst.*, **137**, 1 (1986).

4) I. Moustakali-Mavridis, E. Hadjoudis, and A. Mavridis, *Acta Crystallogr., Sect. B*, **B34**, 3709 (1978).

5) J. I. Bullock, M. F. C. Ladd, D. C. Povey, and H.-A. Tajmir-Riahi, *Acta Crystallogr., Sect. B*, **B35**, 203 (1079).

6) M. E. Kamwaya and L. E. Khoo, *Acta Crystallogr., Sect. C*, **C41**, 1027 (1985).

7) J. W. Ledbetter, Jr., *J. Phys. Chem.*, **81**, 54 (1977).

8) R. Nakagawa, T. Kobayashi, J. Nakamura, and S. Nagakura, *Bull. Chem. Soc. Jpn.*, **50**, 1909 (1977).

9) N. Hoshino, T. Inabe, T. Mitani, and Y. Maruyama, *Bull. Chem. Soc. Jpn.*, **61**, 4207 (1988); T. Inabe, N. Hoshino, T. Mitani, and Y. Maruyama, *Bull. Chem. Soc. Jpn.*, **62**, 2245 (1989).

10) T. Inabe, I. Gautier-Luneau, N. Hoshino, K. Okaniwa, H. Okamoto, T. Mitani, U. Nagashima, and Y. Maruyama, *Bull. Chem. Soc. Jpn.*, **64**, 801 (1991).

11) T. Inabe, I. G. Luneau, T. Mitani, Y. Maruyama, and S. Takeda, *Bull. Chem. Soc. Jpn.*, **67**, 612 (1994); T. Inabe, N. Hoshino-Miyajima, I. G. Luneau, T. Mitani and, Y. Maruyama, *Bull. Chem. Soc. Jpn.*, **67**, 622 (1994).

12) M. Tanaka, H. Hayashi, S. Matsumoto, S. Kashino, and K. Mogi, *Bull. Chem. Soc. Jpn.*, **70**, 329 (1997).

13) H. Hayashi, M. Tanaka, S. Matsumoto, S. Kashino, and K. Mogi, *Mol. Crst. Liq. Crst.*, **286**, 305 (1996).

14) M. Tanaka, H. Matsui, J. Mizoguchi, and S. Kashino, *Bull. Chem. Soc. Jpn.*, **69**, 1572 (1994).

15) M. Tanaka and H. Tsunekawa, *Mol. Crst. Liq. Cryst.*, **313**, 355 (1998).

16) A. I. Vogel, "Practical Organic Chemistry," Longmans, London (1966), p. 653.

17) G. J. Gilmore, *J. Appl. Crystallogr.*, **17**, 42 (1984).

18) "International Tables for X-Ray Crystallography," Kynoch Press, Birmingham (Present distributor Kluwer Academic Publisher, Dordrecht) (1974), Vol. IV, pp. 22—98.

19) "TEXAN. Single Crystal Structure Anlysis Software, Version 5.0," Molecular Structure Corporation, The Woodlands, Texas (1989).

20) List of structure factors, anisotropic displacement parameters for non-H atoms, atomic parameters for H-atoms, and bond lengths and angles for NSAP have been deposited as Document No. 71061 at the Office of the Editor of Bull. Chem. Soc. Jpn. The authors have deposited atomic coordinates for these structures with the Cambridge Crystallographic Data Centre, 12 Union Road, Cambridge CB2 1EZ, UK.

21) M. J. Frisch, G. W. Trucks, H. B. Schlegel, P. M. W. Gill, B. G. Johnson, M. A. Robb, J. R. Cheeseman, T. Keith, G. A. Petersson, J. A. Montgomery, M. A. Al-Laham, V. G. Zakrzewski, J. V. Ortiz, J. B. Foresman, J. Cioslowski, B. B. Stefanov, K. Raghavachari, A. Nanayakkara, M. Challacombe, C. Y. Peng, P. Y. Ayala, W. Chen, M. W. Wong, J. L. Andres, E. S. Replogle, R. Gomperts, R. L. Martin, D. J. Fox, J. S. Binkely, D. J. Defrees, J. Baker, J. P. Stewart, M. Head-Gordon, C. Gonzalez, and J. A. Pople, "Gaussian 94, Revision C," Gaussian, Inc., Pittsburgh PA, USA (1995).

22) C. K. Johnson, "ORTEP II, Report ORNL-5138," Oak Ridge National Laboratory, Tennessee (1976).

23) W. Theilacker, G. Kortum, and G. Friedheim, *Chem. Ber.*, **83**, 508 (1950).

24) M. Tanaka, *Bull. Chem. Soc. Jpn.*, **51**, 1001 (1978).